Available online at www.eccomasproceedia.org
Eccomas Proceedia COMPDYN (2019) 1621-1629

ECCOMAS
Proceedia

COMPDYN 2019
7th ECCOMAS Thematic Conference on
Computational Methods in Structural Dynamics and Earthquake Engineering
M. Papadrakakis, M. Fragiadakis (eds.)
Crete, Greece, 24–26 June 2019

PERFECTLY MATCHED LAYERS FOR THE SIMULATION OF ELASTIC WAVES IN ANISOTROPIC MEDIA

Jun Won Kang[1] and Boyoung Kim[1]

[1] Department of Civil Engineering, Hongik University
Wausan-ro 94, Mapo-gu, Seoul 04066, Republic of Korea
e-mail: jwkang@hongik.ac.kr, by900824@daum.net

Abstract

This paper introduces perfectly matched layers (PMLs) for the simulation of elastic waves in heterogeneous anisotropic media. The PMLs are used as wave-absorbing boundaries to surround a finite computational domain of interest truncated from the originally semi-infinite extent. In the formulation, standard Navier equations governing the wave motion in the regular domain are combined with mixed unsplit-field equations which yield the solution of attenuated waves within the PML. For the modeling of anisotropic material properties, the strain-stress relationship of the anisotropic material is incorporated into the constitutive relation of the mixed unsplit-field wave equations in PML-truncated domains. In this work, a transversely isotropic material is considered for elastic waves in a semi-infinite domain truncated by PML. The second-order semi-discrete form of the problem is constructed by using a mixed finite element method and integrated in time for the solution of displacements and stresses by using the Newmark time integration method. Numerical results are presented for elastic waves propagating in the transversely isotropic PML-truncated domain. The wave motion in the anisotropic medium is compared with that in the corresponding isotropic medium, and the effect of wave attenuation enforced by the developed anisotropic PML is shown by a series of numerical examples.

Keywords: Perfectly Matched Layers, Elastic Waves, Anisotropic Media, Mixed Finite Element Method, Time Integration.

Peer-review under responsibility of the organizing committee of COMPDYN 2019.
doi: 10.7712/120119.7023.19063

1 INTRODUCTION

Elastic wave propagation in anisotropic media is important in many branches of applied engineering and sciences such as structural mechanics, geophysics, and petroleum engineering. In anisotropic media, waves propagate with different speeds in different directions. The material anisotropy is comparatively common and could be caused by various mechanisms including crystal alignment, stress-induced effect, regular placement of fine layers, and aligned cracks [1]. For simulation of elastic waves in such domains, there have been many developments in the theory and calculation of wave propagation in anisotropic media [2, 3]. Most of the wave implementations are based on finite-difference-time-domain (FDTD) methods on staggered grids. However, the staggered grid approach is challenging to implement for general aniso-tropic materials, especially in curvilinear coordinates, and may be subject to stability issues. As an effort to relieve this problem, second-order displacement formulations with finite element or spectral element methods have been used for modeling general anisotropy [2].

Another challenge in the wave simulation is to implement absorbing boundary conditions for anisotropic unbounded elastic media. A useful way to achieve this is to use perfectly matched layers (PMLs), which surround a finite region of interest truncated from the unbounded domain and attenuate outgoing waves from the interior of the domain. Despite some stability issues, the PML is considered to be one of the most accurate absorbing boundary conditions available. To implement the PML in anisotropic media, several PML methods such as Convolutional PML(C-PML) and unsplit C-PML were developed, which improve dynam-ical stability of the classical PML method [4, 5]. The C-PML, however, requires special treat-ment for evaluating the costly convolutional integral. Assi and Cobbold [6] also improved the stability of PML for anisotropic elastic media while reducing the computational cost, but the formulation requires four auxiliary equations, which increase implementation complexity. In recent years, an unsplit-field displacement-stress formulation of PML was proposed in the time domain, resulting in accurate and stable solutions with a straightforward approach for integrating in time the second-order semi-discrete form [7-9].

This work improves on the earlier mixed unsplit-field formulation by incorporating material anisotropy into the mixed unsplit-field wave equations for PML-truncated domains. A transversely isotropic material is considered for the anisotropic medium, and the numerical results are presented for elastic waves propagating in the transversely isotropic PML-truncated domain. The series of examples show the effect of the developed PML method for attenuating waves in anisotropic elastic media.

2 ELASTIC WAVES IN A PML-TRUNCATED DOMAIN

2.1 Complex coordinate stretching

For the wave simulation in a semi-infinite domain, the original extent can be modeled as a PML-truncated domain as shown in Figure 1. The domain consists of a regular domain (Ω_{reg}) and the surrounding PML (Ω_{PML}). In this setting, a complex coordinate stretching can be defined as a change of coordinates from a real space to an imaginary space:

$$\tilde{s} = \int_0^s \varepsilon_s(s', \omega) ds', \quad \varepsilon_s(s, \omega) = \alpha_s(s) + \frac{\beta_s(s)}{i\omega} \tag{1}$$

where $s(= x, y)$ denotes real coordinates, ω is frequency, and i is the imaginary unit. $\tilde{s}$ is a complex-valued virtual coordinate transformed from s by integrating a stretching function, ε_S, which consists of wave attenuation functions, α_s and β_s. In the regular domain, the attenuation functions are defined as $\alpha_s = 1$ and $\beta_s = 0$, whereas in PML, they can be written as [7, 8]

$$\alpha_s = 1 + \frac{3b}{2L_s^{\mathrm{PML}}}\log\left(\frac{1}{|R|}\right)\left[\frac{(s-s_0)n_s}{L_s^{\mathrm{PML}}}\right]^2, \quad \beta_s = \frac{3c_p^{\mathrm{ref}}}{2L_s^{\mathrm{PML}}}\log\left(\frac{1}{|R|}\right)\left[\frac{(s-s_0)n_s}{L_s^{\mathrm{PML}}}\right]^2 \tag{2}$$

where L_s^{PML} denotes the length of PML in the s-direction, b is the characteristic length of the domain, and s_0 is the location of interface between regular and PML domains. R is a complex-valued user-tunable reflection coefficient, and n_s is the s-directional component of the unit normal vector on the interface. It has been shown that, by introducing the stretched coordinate, the waveform, $\exp(-ik\tilde{\mathbf{x}}\cdot\mathbf{d})$, decays exponentially [7-9]. Therefore, by reformulating wave equations with the coordinate stretching, one can accomplish artificial wave attenuation in the PML.

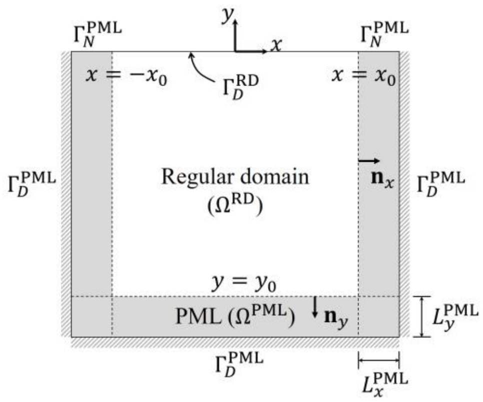

Figure 1: A two-dimensional PML-truncated domain

2.2 Governing equations

By applying the coordinate stretching to equilibrium, constitutive, and compatibility equations in elastodynamics, the following coupled partial differential equations governing elastic waves in PML-truncated domains can be obtained [9]:

$$\mathrm{div}\left(\dot{\mathbf{S}}^{\mathrm{T}}\widetilde{\mathbf{\Lambda}}_e + \mathbf{S}^{\mathrm{T}}\widetilde{\mathbf{\Lambda}}_p\right) + a\dot{\mathbf{f}} = \rho(a\ddot{\mathbf{u}} + b\dot{\mathbf{u}} + c\mathbf{u}) \tag{3}$$

$$\begin{aligned} &\mathbf{\Lambda}_e^{\mathrm{T}}(\mathbf{D}:\ddot{\mathbf{S}})\mathbf{\Lambda}_e + \mathbf{\Lambda}_e^{\mathrm{T}}(\mathbf{D}:\dot{\mathbf{S}})\mathbf{\Lambda}_p + \mathbf{\Lambda}_p^{\mathrm{T}}(\mathbf{D}:\dot{\mathbf{S}})\mathbf{\Lambda}_e + \mathbf{\Lambda}_p^{\mathrm{T}}(\mathbf{D}:\mathbf{S})\mathbf{\Lambda}_p \\ &= \frac{1}{2}\left\{\mathbf{\Lambda}_p^{\mathrm{T}}(\nabla\mathbf{u}) + (\nabla\mathbf{u})^{\mathrm{T}}\mathbf{\Lambda}_p + \mathbf{\Lambda}_e^{\mathrm{T}}(\nabla\dot{\mathbf{u}}) + (\nabla\dot{\mathbf{u}})^{\mathrm{T}}\mathbf{\Lambda}_e\right\} \end{aligned} \tag{4}$$

where $\mathbf{u} = \left[u_x\ u_y\right]^{\mathrm{T}}$ denotes displacements, $\mathbf{S} = \int_0^t \boldsymbol{\sigma}(\mathbf{x},\tau)d\tau$ the stress memory, and $\mathbf{E} = \int_0^t \boldsymbol{\epsilon}(\mathbf{x},\tau)d\tau$ the strain memory. $\mathbf{f}$ denotes body force, ρ is medium density, and $\mathbf{D}$ is the elastic compliance tensor. The coefficients a, b, and c are represented in terms of wave attenuation functions as $a = \alpha_x\alpha_y$, $\beta = \alpha_x\beta_y + \beta_x\alpha_y$, and $c = \beta_x\beta_y$. The stretching tensors $\mathbf{\Lambda}_e$ and $\mathbf{\Lambda}_p$ are written in terms of the stretching functions as

$$\mathbf{\Lambda}^{-1} = \begin{bmatrix}\varepsilon_x & 0\\ 0 & \varepsilon_y\end{bmatrix} = \begin{bmatrix}\alpha_x & 0\\ 0 & \alpha_y\end{bmatrix} + \frac{1}{i\omega}\begin{bmatrix}\beta_x & 0\\ 0 & \beta_y\end{bmatrix} = \mathbf{\Lambda}_e + \frac{1}{i\omega}\mathbf{\Lambda}_p \tag{5}$$

$$\widetilde{\mathbf{\Lambda}} = \begin{bmatrix}\varepsilon_y & 0\\ 0 & \varepsilon_x\end{bmatrix} = \begin{bmatrix}\alpha_y & 0\\ 0 & \alpha_x\end{bmatrix} + \frac{1}{i\omega}\begin{bmatrix}\beta_y & 0\\ 0 & \beta_x\end{bmatrix} = \widetilde{\mathbf{\Lambda}}_e + \frac{1}{i\omega}\widetilde{\mathbf{\Lambda}}_p \tag{6}$$

3 ANISOTROPIC MATERIAL MODELING

To consider material anisotropy in the PML-truncated domain, the elastic compliance tensor, **D**, in Eqs. (3) and (4) can be modified appropriately. In this work, a transversely isotropic material is considered for the elastic waves in the PML-truncated domain. The strain-stress relationship of a transversely isotropic medium in three-dimensions can be written as follows:

$$\begin{bmatrix} \epsilon_x \\ \epsilon_y \\ \epsilon_z \\ \epsilon_{yz} \\ \epsilon_{zx} \\ \epsilon_{xy} \end{bmatrix} = \begin{bmatrix} \frac{1}{E_T} & -\frac{\nu_{LT}}{E_L} & -\frac{\nu_{TT}}{E_T} & 0 & 0 & 0 \\ -\frac{\nu_{TL}}{E_T} & \frac{1}{E_L} & -\frac{\nu_{TL}}{E_T} & 0 & 0 & 0 \\ -\frac{\nu_{TT}}{E_T} & -\frac{\nu_{LT}}{E_L} & \frac{1}{E_T} & 0 & 0 & 0 \\ 0 & 0 & 0 & \frac{1}{2\mu_{LT}} & 0 & 0 \\ 0 & 0 & 0 & 0 & \frac{1}{2\mu_{TT}} & 0 \\ 0 & 0 & 0 & 0 & 0 & \frac{1}{2\mu_{TL}} \end{bmatrix} \begin{bmatrix} \sigma_x \\ \sigma_y \\ \sigma_z \\ \sigma_{yz} \\ \sigma_{zx} \\ \sigma_{xy} \end{bmatrix} \quad (7)$$

where xz-plane is the plane of isotropy, and the y-axis is the symmetric axis that is normal to the plane of isotropy. The elastic moduli and Poisson's ratios in the transverse and longitudinal directions are written as

$$E_x = E_z = E_T, \quad \mu_{xz} = \mu_{TT}, \quad \nu_{xz} = \nu_{zx} = \nu_{TT} \quad (8)$$

$$E_z \neq E_y = E_L, \quad \mu_{yz} = \mu_{xz} = \mu_{TL}, \quad \nu_{yz}(= \nu_{LT}) \neq \nu_{zy}(= \nu_{TL}) \quad (9)$$

Assuming a plane strain condition where strains along the z-direction are zero, the constitutive relationship, $\mathbf{E} = \mathbf{D}:\mathbf{S}$, in Eq. (7) can be reduced to

$$\begin{bmatrix} \epsilon_x \\ \epsilon_y \\ \epsilon_{xy} \end{bmatrix} = \begin{bmatrix} Q_{11} & Q_{12} & 0 \\ Q_{21} & Q_{22} & 0 \\ 0 & 0 & Q_{33} \end{bmatrix} \begin{bmatrix} \sigma_x \\ \sigma_y \\ \sigma_{xy} \end{bmatrix} \quad (10)$$

in which the components of the two-dimensional compliance matrix are written as

$$Q_{11} = \frac{1-\nu_{xz}^2}{E_x}, \quad Q_{12} = Q_{21} = -\frac{\nu_{xy}(1+\nu_{xz})}{E_x}, \quad Q_{22} = \frac{1-\nu_{xy}\nu_{yx}}{E_y}, \quad Q_{33} = \frac{1}{2\mu_{xy}} \quad (11)$$

By substituting Eqs. (10) and (11) into Eq. (4), one can mathematically model transient elastic waves in a transversely isotropic medium truncated by PMLs.

4 THE WEAK FORM AND A MIXED FINITE ELEMENT METHOD

The coupled equations (3) and (4) can be solved for displacements **u** and stress memories **S** by using a mixed finite element method. For the construction of the weak form of Eq. (3), both sides of the equation are dotted with a test function vector for displacement and integrated over the entire domain. Similarly, the weak form of Eq. (4) can be obtained by taking the dot product of the equation and a test function tensor for stress memory and integrating over the same domain. There result

$$\begin{aligned}&\int_{\Omega} \nabla\mathbf{w}:\left(\dot{\mathbf{S}}^{\mathrm{T}}\widetilde{\mathbf{\Lambda}}_e+\mathbf{S}^{\mathrm{T}}\widetilde{\mathbf{\Lambda}}_p\right)d\Omega+\int_{\Omega} \mathbf{w}\cdot\rho(a\ddot{\mathbf{u}}+b\dot{\mathbf{u}}+c\mathbf{u})d\Omega\\&=\int_{\Gamma_N} \mathbf{w}\cdot\left(\dot{\mathbf{S}}^{\mathrm{T}}\widetilde{\mathbf{\Lambda}}_e+\mathbf{S}^{\mathrm{T}}\widetilde{\mathbf{\Lambda}}_p\right)\mathbf{n}d\Gamma+\int_{\Gamma_N} \mathbf{w}\cdot a\mathbf{f}d\Gamma\end{aligned} \tag{12}$$

$$\begin{aligned}&\int_{\Omega}\left(\mathbf{D}:\ddot{\mathbf{S}}\right):\left(\mathbf{\Lambda}_e\mathbf{T}\mathbf{\Lambda}_e^{\mathrm{T}}\right)d\Omega+\int_{\Omega}\left(\mathbf{D}:\dot{\mathbf{S}}\right):\left(\mathbf{\Lambda}_e\mathbf{T}\mathbf{\Lambda}_p^{\mathrm{T}}+\mathbf{\Lambda}_p\mathbf{T}\mathbf{\Lambda}_e^{\mathrm{T}}\right)d\Omega+\int_{\Omega}(\mathbf{D}:\mathbf{S}):\left(\mathbf{\Lambda}_p\mathbf{T}\mathbf{\Lambda}_p^{\mathrm{T}}\right)d\Omega\\&=\int_{\Omega} \nabla\mathbf{u}:\mathbf{\Lambda}_p\mathbf{T}d\Omega+\int_{\Omega} \nabla\dot{\mathbf{u}}:\mathbf{\Lambda}_e\mathbf{T}d\Omega\end{aligned} \tag{13}$$

where **w** and **T** are the test function vector for displacement and the test function tensor for stress memory, respectively. The constitutive relationship of Eqs. (10) and (11) is implicitly imposed in the weak form to consider material anisotropy. The symbols Ω and Γ_N denote the PML-truncated domain and its Neumann boundary, respectively, as shown in Figure 1. In arriving at Eq. (12), the divergence theorem has been applied. For spatial discretization of the displacement and the stress memory in Eqs. (12) and (13), a mixed finite element method can be used, where the order of basis functions for the two variables are significant for the stability of solutions. In this work, using quadratic basis functions with a serendipity element for both displacement and stress memory yielded stable solutions. After introducing the spatial discretization to the weak forms, semi-discrete equations of motion could be derived, and the numerical solution was calculated by using the Newmark time integration method.

5 NUMERICAL EXAMPLES

As an illustrative example of the anisotropic unsplit-field PML, a PML-truncated semi-infinite domain of a transversely isotropic material, as shown in Figure 2, is considered. The size of the regular domain is 12 m × 12 m, and the PML is 2 m wide. The domain is homogeneous with density $\rho = 2000\ \mathrm{kg/m^3}$, $E_x = 200$ MPa, $E_y = 300$ MPa, $\mu_{xy} = 83.33$ MPa, $\nu_{xy} = 0.2$, and $\nu_{yx} = 0.3$. The combined regular and PML domains are discretized using biquadratic elements with an element size of 0.05 m. There result 40 elements within each PML region. A reflection coefficient of $|R| = 10^{-8}$ is used for the PML. As an excitation to the domain, a stress load $\sigma_{22} = p(t)$ in the form of a Ricker pulse is applied over a small region (-0.2 m $\leq x \leq$ 0.2 m) on the surface of the domain. The central frequency of the Ricker pulse is 100 Hz as shown in Figure 3, and the time step is 0.0005 s.

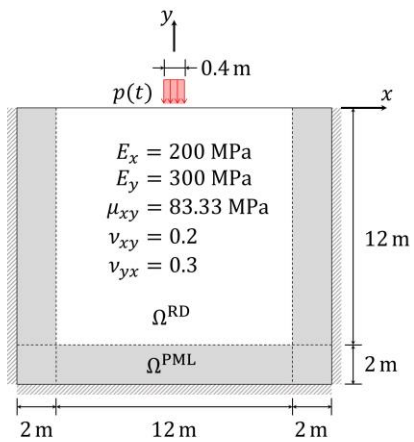

Figure 2: A PML-truncated domain of a transversely isotropic material

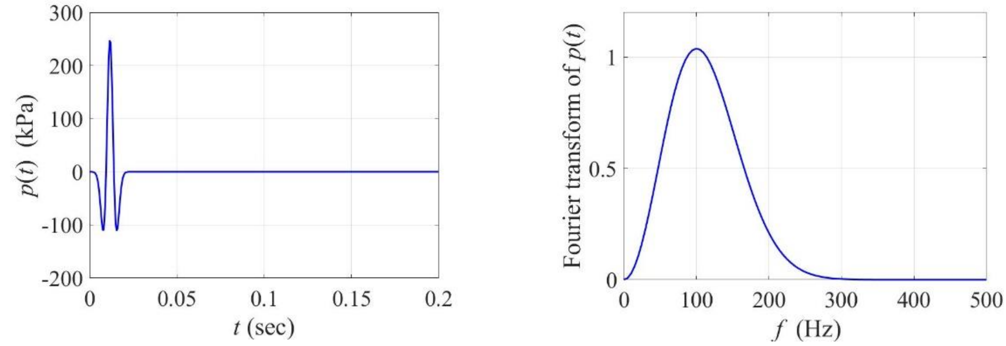

(a) Time history (b) Frequency spectrum

Figure 3: Excitation signal and its Fourier spectrum

Figure 4(a) shows displacement waves at $t = 0.035$ s due to the surface load in the transversely isotropic medium. As can be seen in the figure, there are no discernable reflections propagating back to the regular domain. The displacement is continuous at the interface between the regular and PML regions, and the waves are attenuated rapidly with distance to the layer. For comparison, displacement waves in the corresponding isotropic medium at the same time instant are presented in Figure 4(b). The isotropic medium has the Young's modulus of 200 MPa and the Poisson's ratio of 0.2. Since, in the anisotropic medium, the elastic modulus in the y-direction is 1.5 times that in the x-direction, the waves propagate faster in the y-direction than in the other direction, as shown in Figure 4. Figure 5(a) presents the time history of displacement at the coordinate point (0,-12), located at the interface between the regular domain and bottom PML. The waves reach the point earlier in the case of the transversely isotropic medium than in the case of the isotropic domain. Figure 5(b) shows the snapshot of u_y at $t = 0.023$ s along the line of $x = 0$. It can be seen that compressional waves travel faster in the anisotropic medium than in the isotropic medium.

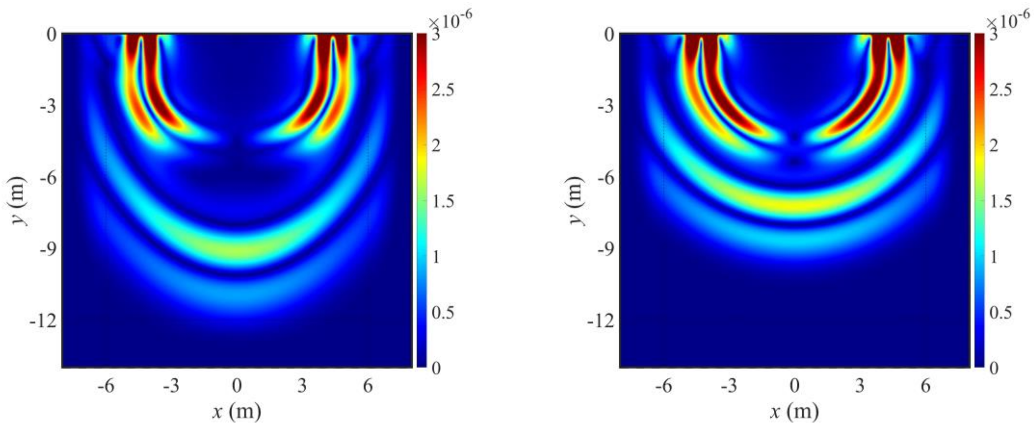

(a) (b)

Figure 4: Displacement waves at $\boldsymbol{t = 0.035}$ s due to the surface load in (a) the transversely isotropic medium and (b) the isotropic medium

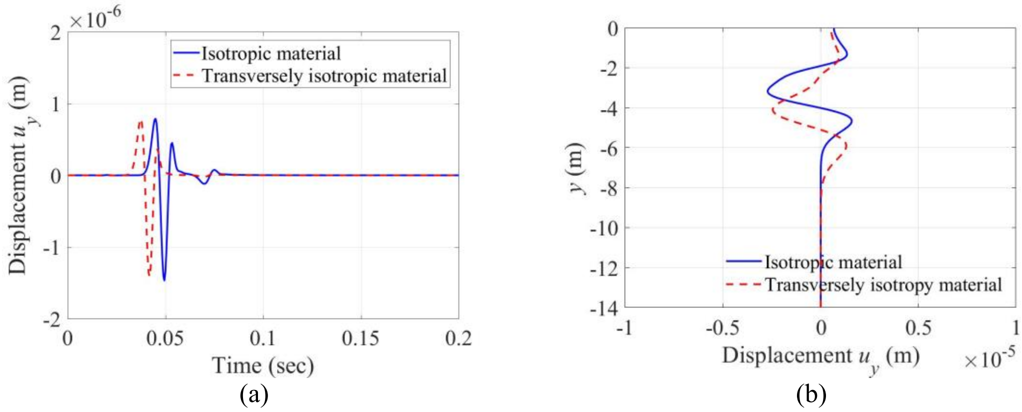

Figure 5: Displacement $\boldsymbol{u_y}$ in the anisotropic and isotropic media; (a) time history of the displacement at the point of coordinates (0,-12) and (b) the snapshot of $\boldsymbol{u_y}$ at $\boldsymbol{t = 0.023}$ s along the line of $\boldsymbol{x = 0}$

The proposed unsplit-field PML method can also be applied to heterogeneous anisotropic media. For demonstration, elastic wave propagation in a PML-truncated domain shown in Figure 6(a) is considered. The size of regular and PML domains is the same as the previous case, but the medium is stratified to two layers with material property values shown in the figure. Figure 6(b) depicts displacement waves propagating in the heterogeneous anisotropic domain due to the surface excitation presented in Figure 3. Compared to the homogeneous domain case in Figure 4(a), some of the waves are reflected back to the surface at the interface between the two layers, and the rest are transmitted into the lower layer. No discernable reflections from the PML can be found in this case as well. Figure 7 presents the time history of u_y at coordinate points (0,0) and (0,-12). The waves in the heterogeneous medium reach the bottom point earlier than those in the homogeneous medium because of the increase of E_y in the second layer. The time history shows a few reflections caused by the layer interface, but they disappear as the waves travel back and forth several times within the domain.

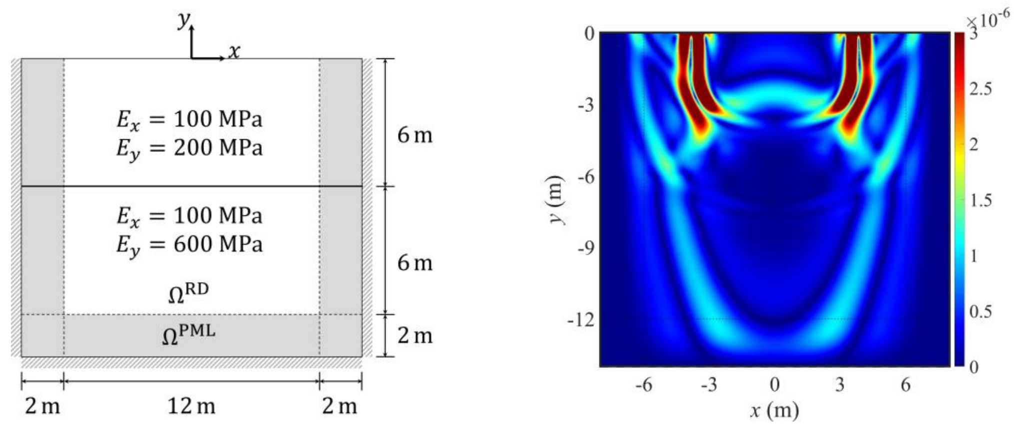

Figure 6: Results of elastic wave simulation in a heterogeneous anisotropic PML-truncated domain; (a) a two-layer profile and (b) the snapshot of displacement at $\boldsymbol{t = 0.04}$ s

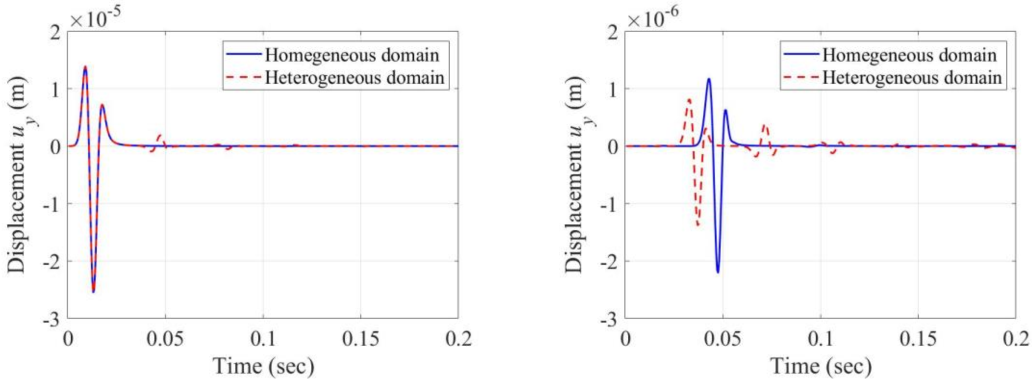

(a) Point (0,0) (b) Point (0,-12)

Figure 7: Time history of $\boldsymbol{u_y}$ in the heterogeneous and homogeneous media; both media are transversely isotropic

6 CONCLUSIONS

- A mixed unsplit-field PML method has been developed for the simulation of elastic waves in unbounded anisotropic media.
- For the modeling of anisotropic material properties, the strain-stress relationship of the anisotropic material can be incorporated into the constitutive relation of the mixed unsplit-field wave equations in PML-truncated domains.
- The unsplit-field wave equations in anisotropic PML-truncated domains can be implemented by a mixed finite element method. In this work, a transversely isotropic material is considered for elastic waves in a semi-infinite domain truncated by PML. It has been found that the numerical solution is continuous at the interface between the regular and PML domains, and there are no discernable reflections propagating back to the regular domain.
- The proposed unsplit-field PML method for anisotropic media can also be applied to heterogeneous domains. The method captures well the reflection and transmission of elastic waves at the interface of material layers, while eliminating the waves within PML effectively.

REFERENCES

[1] S. Crampin, A review of wave motion in anisotropic and cracked elastic-media, *Wave Motion 3*, 343–391, 1981.

[2] N. Petersson, B. Sjögreen, Wave propagation in anisotropic elastic materials and curvilinear coordinates using a summation-by-parts finite difference method, *Journal of Computational Physics*, **299**(15), 820-841, 2015.

[3] M.D. Sharma, Three-dimensional wave propagation in a general anisotropic poroelastic medium: phase velocity, group velocity and polarization, *Geophysical Journal International*, **156**, 329-344, 2004.

[4] M. Kuzuoglu, R. Mittra, Frequency dependence of the constitutive parameters of causal perfectly matched anisotropic absorbers, *IEEE Microwave and Guided wave letters*, **6**(12), 447-449, 1996.

[5] D. Komatitsch, R. Martin, An unsplit convolutional perfectly matched layer improved at grazing incidence for the seismic wave equation, *Geophysics*, **72**(5), SM155-SM167, 2007.

[6] H. Assi, R. Cobbold, Perfectly matched layer for second-order time-domain elastic wave equation: formulation and stability, *arXiv preprint arXiv*, 1312-3722, 2013.

[7] J.W. Kang, L.F. Kallivokas, Mixed unsplit-field perfectly matched layers for transient simulations of scalar waves in heterogeneous domains, *Computational Geosciences*, **14**(4), 623-648, 2010.

[8] A. Pakravan, J.W. Kang, C.M. Newtson, L.F. Kallivokas, Hybrid perfectly-matched-layers for transient simulation of scalar elastic waves, *Structural Engineering and Mechanics*, **51**(4), 685-705, 2014.

[9] A. Fathi, L.F. Kallivokas, B. Poursartip, Full-waveform inversion in three-dimensional PML-truncated elastic media, *Computer Methods in Applied Mechanics and Engineering*, **296**, 39–72, 2015.